

See discussions, stats, and author profiles for this publication at: <https://www.researchgate.net/publication/225188342>

# Surface Speciation Models of Calcite and Dolomite/Aqueous Solution Interfaces and Their Spectroscopic Evaluation

ARTICLE in *LANGMUIR* · MARCH 2000

Impact Factor: 4.46 · DOI: 10.1021/la980905e

CITATIONS

101

READS

115

## 4 AUTHORS:



**Oleg S. Pokrovsky**

GET UMR 5563 CNRS, IEPS RAS Arkhangelsk, ...

243 PUBLICATIONS 4,905 CITATIONS

SEE PROFILE



**Jerzy A Mielczarski**

University of Lorraine

58 PUBLICATIONS 1,680 CITATIONS

SEE PROFILE



**Barrès Odile**

University of Lorraine

93 PUBLICATIONS 1,543 CITATIONS

SEE PROFILE



**Jacques Schott**

French National Centre for Scientific Research

237 PUBLICATIONS 9,255 CITATIONS

SEE PROFILE

# Surface Speciation Models of Calcite and Dolomite/Aqueous Solution Interfaces and Their Spectroscopic Evaluation

O. S. Pokrovsky,<sup>†</sup> J. A. Mielczarski,<sup>\*,‡</sup> O. Barres,<sup>‡</sup> and J. Schott<sup>†</sup>

Laboratoire de Géochimie, UPS-CNRS (UMR 5563) 38, Rue des Trente-Six Ponts, 31400, Toulouse, France, and Laboratoire Environnement et Minéralurgie UMR 7569 CNRS, INPL-ENSG, B.P. 40, 54501 Vandoeuvre-les-Nancy Cedex, France

Received July 17, 1998. In Final Form: November 8, 1999

The composition and density of surface hydroxyl and carbonate groups on calcite and dolomite after contact at 25 °C with solutions of different pH (3 to 12) and carbonate concentration ( $10^{-4} \leq \Sigma\text{CO}_2 \leq 0.1$  M) were monitored by means of diffuse reflectance infrared (DRIFT) spectroscopy. Both for calcite and dolomite, broad high-intensity absorbance bands at about 3400 and 1600  $\text{cm}^{-1}$  were observed at pH below 6 and carbonate concentration below  $10^{-3}$  M. These bands are assigned to hydroxyl groups present at the mineral surfaces. At higher pH and  $\Sigma\text{CO}_2$ , the intensity of these bands significantly decreases. On the contrary the intensity of the broad double band at about 1400  $\text{cm}^{-1}$  due to carbonate species (surface and bulk) for both minerals was found to increase significantly with increasing solution pH and carbonate concentration, being the lowest at pH  $\leq 5$  and  $\Sigma\text{CO}_2 \leq 10^{-3}$  M. These observations correlate well with the surface speciation for calcite or dolomite/aqueous solution interface predicted based on surface complexation models (SCM). These models were proposed based on the electrokinetics and surface titration experimental results and they postulate the formation of  $>\text{CaOH}_2^+$ ,  $>\text{MgOH}_2^+$ ,  $>\text{CaHCO}_3^0$ ,  $>\text{MgHCO}_3^0$ ,  $>\text{CaCO}_3^-$ ,  $>\text{MgCO}_3^-$ ,  $>\text{CO}_3\text{Ca}^+$ ,  $>\text{CO}_3\text{Mg}^+$ , and  $>\text{CO}_3^-$  surface species from two primary hydration sites,  $>\text{CaOH}^0$  ( $>\text{MgOH}^0$ ) and  $>\text{CO}_3\text{H}^0$ . Very good relationships were found between the predicted concentration of the surface OH groups ( $>\text{MeOH}_2^+$ ) and the measured density of the surface hydroxyl groups corresponding to a band at around 3400  $\text{cm}^{-1}$ . Moreover, the experimental ratio of band intensities  $I_{3400}/I_{1420}$  (OH/CO<sub>3</sub>) was found to correlate well with the predicted concentration ratio of the adsorbed surface hydroxyl and carbonate groups,  $\{>\text{MeOH}_2^+\}/\{>\text{MeHCO}_3^0 + >\text{MeCO}_3^-\}$ . External addition of  $\text{Mg}^{2+}$  or  $\text{Ca}^{2+}$  ions to alkaline dolomite suspensions leads to an increase of the surface density of the OH groups. This increase is explained, in accordance with the SCM, by the formation of  $>\text{CO}_3\text{Me}^+ \times n\text{H}_2\text{O}$  outer sphere species that yield an increase of surface adsorbed water.

## Introduction

Calcium and magnesium carbonates comprise about 21% of the sedimentary crust. Consequently, the reactivity of these minerals (adsorption, dissolution/precipitation phenomena) controls most surficial processes such as weathering rates, the fate of contaminants, scavenging of many elements in the ocean, and the composition of soil solutions and groundwater. All these phenomena are controlled by chemical processes taking place at the interface between the mineral lattice and the bulk solution. During the past decade, considerable progress has been made in the characterization of calcium carbonate surface chemistry,<sup>1–5</sup> studying dissolution/precipitation phenomena,<sup>6–15</sup> and sorption/incorporation of aqueous ions<sup>16–24</sup>

and organic molecules.<sup>25–27</sup> However, the identity and structure of the actual surface species controlling the processes on the carbonate/aqueous solution interface remain poorly known and are subject to controversy. A better understanding of the surface composition of carbonate minerals can be obtained by combining spectro-

\* Corresponding author.

<sup>†</sup> Laboratoire de Géochimie.

<sup>‡</sup> Laboratoire Environnement et Minéralurgie.

(1) Thompson, D. W.; Pownall, P. G. *J. Colloid Interface Sci.* **1989**, *131*, 74.

(2) Huang, Y. C.; Fowkes, F. M.; Lloyd, T. B.; Sanders, N. D. *Langmuir* **1991**, *7*, 1742.

(3) Cicerone, D. S.; Regazzoni, A. E.; Blesa, M. A. *J. Colloid Interface Sci.* **1992**, *154*, 423.

(4) de Leeuw, N. H.; Parker, S. C. *J. Chem. Soc., Faraday Trans.* **1997**, *93*, 467.

(5) Titiloye, J. O.; de Leeuw, N. H.; Parker, S. C. *Geochim. Cosmochim. Acta* **1998**, *62*, 2637.

(6) Chou, L.; Garrels, R. M.; Wollast, R. *Chem. Geology* **1989**, *78*, 269.

(7) Gratz, A. J.; Hillner, P. E.; Hansma, P. K. *Geochim. Cosmochim. Acta* **1993**, *57*, 491.

(8) Brown, C. A.; Compton, R. G.; Narramore, C. A. *J. Colloid Interface Sci.* **1993**, *160*, 372.

(9) Compton, R. G.; Brown, C. A. *J. Colloid Interface Sci.* **1994**, *165*, 445.

(10) Compton, R. G.; Brown, C. A. *J. Colloid Interface Sci.* **1995**, *170*, 586.

(11) Park, N.-S.; Kim, M.-W.; Langford, S. C.; Dickinson, J. T. *Langmuir* **1996**, *12*, 4599.

(12) Liang, Y.; Baer, D. R. *Surf. Sci.* **1997**, *373*, 275–287.

(13) McCoy, J. M.; LaFemina, J. P. *Surf. Sci.* **1997**, *373*, 288–299.

(14) Jordan, G.; Rammensee, W. *Geochim. Cosmochim. Acta* **1998**, *62*, 941.

(15) Pokrovsky, O. S. *J. Crystal Growth* **1998**, *186*, 233.

(16) Zachara, J. M.; Cowan, C. E.; Resch, C. T. *Geochim. Cosmochim. Acta* **1991**, *55*, 1549.

(17) Zhong, S.; Mucci, A. *Geochim. Cosmochim. Acta* **1995**, *59*, 443.

(18) Paquette, J.; Reeder, R. J. *Geochim. Cosmochim. Acta* **1995**, *59*, 735.

(19) Brady, P. V.; Krumhansl, J. L.; Papenguth, H. W. *Geochim. Cosmochim. Acta* **1996**, *60*, 727.

(20) Reeder, R. J. *Geochim. Cosmochim. Acta* **1996**, *60*, 1543.

(21) Tesoriero, A.; Pankow, J. *Geochim. Cosmochim. Acta* **1996**, *60*, 1053.

(22) Watson, E. B. *Geochim. Cosmochim. Acta* **1996**, *60*, 5013.

(23) Hemming, N. C.; Reeder, R. J.; Hart, S. R. *Geochim. Cosmochim. Acta* **1998**, *62*, 2915.

(24) Rimstidt, J. D.; Balog, A.; Webb, J. *Geochim. Cosmochim. Acta* **1998**, *62*, 1851.

(25) Giannimaras, Geffroy C.; Foissy, A.; Persello, J.; Cabane, B. *J. Colloid Interface Sci.* **1999**, *211*, 45.

(26) Berman, A.; Ahn, D. L.; Lio, A.; Salmeron, M.; Reichert, A.; Charych, D. *Science* **1995**, *269*, 515.

(27) Teng, H.; Dove, P. *Am. Mineral.* **1997**, *82*, 878.

scopic surface information with surface complexation equilibria. The current study presents a direct infrared (IR) spectroscopy observation of surface hydroxyl and carbonate groups on calcite and dolomite exposed to different aqueous solutions and its thermodynamic interpretation.

Owing to the development of surface sensitive spectroscopic techniques such as X-ray photoelectron spectroscopy (XPS), low energy electron diffraction (LEED), atomic force microscopy (AFM), and X-ray absorption spectroscopy (XAS),<sup>28–36</sup> direct atomic-level information on bonding environments at the carbonate mineral/water interface has become available. The first XPS study proved the presence of the hydrolysis species  $>\text{CaOH}^0$  and  $>\text{CO}_3\text{H}^0$  (where  $>$  represents the mineral surface) on the  $\text{CaCO}_3$  surface in contact with humid air and water.<sup>28</sup> A LEED study of the calcite cleavage surface exposed to solution indicated that the top few atomic layers, which exhibit long range order and lattice spacing at the surface, are statistically identical to those of bulk calcite, although slight twisting of surface  $\text{CO}_3$  groups is possible.<sup>28</sup> This was further confirmed by in situ AFM studies of calcite surfaces in water.<sup>31,34</sup> Recently, it has been shown that other in situ measurement techniques, such as synchrotron X-ray standing wave (XSW), X-ray reflectivity, and X-ray scattering (refs 35 and 36, and references therein) can yield precise high-resolution information on the long-range atomic-scale structure, microtopography, and composition of calcite–water interfaces as well as precise surface location and coordination environment of adsorbed metal ions. However, up to the present time, no attempt has been made to quantify the chemical composition of carbonate mineral surfaces as a function of aqueous solution composition using spectroscopic techniques.

In this regard, IR spectroscopy can be a very promising complementary method to widely used XPS, AFM, and XAS techniques in providing detailed information on molecular groups as well as small changes in the environment of the monitored surface groups. Moreover, an infrared beam interacts with the investigated sample very gently (at the level of a part of an eV), and, unlike XPS, does not require ultrahigh vacuum conditions. As a result, the surface composition remains practically unchanged during the spectroscopic investigation compared to the conditions in aqueous solution. Indeed, infrared spectroscopy has long been a useful technique for detecting surface groups on solid surfaces,<sup>37,38</sup> in particular, direct detection of OH groups on oxides and feldspars,<sup>39–43</sup> acidic

and alkaline sites on  $\text{ZnS}$ ,<sup>44</sup> hydroxyl, carbonate, phosphate, and sulfate groups on iron oxy/hydroxides,<sup>45–51</sup> and the study of organic molecule interactions with the surface of calcium minerals.<sup>52–57</sup> Yet, direct detection of the different surface OH and  $\text{CO}_3$  groups produced on calcium and magnesium carbonate surfaces after contact with aqueous solution by infrared spectroscopy has not previously been reported.

Based on the surface titration and electrokinetic study of  $\text{MnCO}_3$ ,  $\text{FeCO}_3$ ,  $\text{MgCO}_3$ , and  $\text{CaMg}(\text{CO}_3)_2$ ,<sup>58,59</sup> surface complexation models (SCMs) of carbonate minerals were developed<sup>59–61</sup> which postulate, in agreement with previous results of spectroscopic investigations,<sup>28,34</sup> the formation of the two primary hydration sites,  $>\text{MeOH}^0$  and  $>\text{CO}_3\text{H}^0$  ( $\text{Me} = \text{Ca}^{2+}$ ,  $\text{Mg}^{2+}$ ), having a 1:1 stoichiometry on the surface. The application of these models for the interpretation of  $\text{CaCO}_3$ ,<sup>62,63</sup>  $\text{MnCO}_3$ ,<sup>64</sup> and  $\text{MgCO}_3$ <sup>65</sup> reactivity in aquatic systems demonstrated their validity in describing the speciation at the carbonate/water interface. Within the framework of SCM, the following species are assumed to form on the metal and carbonate sites exposed to the aqueous solution:  $>\text{MeOH}_2^+$ ,  $>\text{MeOH}^0$ ,  $>\text{MeO}^-$ ,  $>\text{MeHCO}_3^0$ ,  $>\text{MeCO}_3^-$ ,  $>\text{CO}_3\text{Me}^+$ ,  $>\text{CO}_3^-$ , and  $>\text{CO}_3\text{H}^0$ . These surface groups have been inferred indirectly from surface titration, electrokinetics, and dissolution rate studies and from analogies between the surface and aqueous species.<sup>66</sup> The equilibria between these surface groups and aqueous species are described using a set of intrinsic thermodynamic stability constants.

Such a thermodynamic model of the carbonate/solution interface, being derived mostly from the results of macroscopic techniques, requires independent evaluation on the microscopic scale. That is why in this study we attempted to correlate the relative amount of the different

(28) Stipp, S. L.; Hochella, M. F., Jr. *Geochim. Cosmochim. Acta* **1991**, *55*, 1723.

(29) Hillner, P. E.; Manne, S.; Gratz, A. J.; Hansma, P. K. *Ultramicroscopy* **1992**, *42–44*, 1387.

(30) Hillner, P. E.; Gratz, A. J.; Manne, S.; Hansma, P. K. *Geology* **1992**, *20*, 359.

(31) Rachlin, A. L.; Henderson, G. S.; Goh, M. C. *Am. Mineral.* **1992**, *77*, 904.

(32) Dove, P. M.; Hochella, M. F., Jr. *Geochim. Cosmochim. Acta* **1993**, *57*, 705.

(33) Ohnesorge, F.; Binnig, G. *Science* **1993**, *260*, 1451.

(34) Stipp, S. L.; Eggleston, C. M.; Nielsen, B. S. *Geochim. Cosmochim. Acta* **1994**, *58*, 3023.

(35) Chiarello, R. P.; Sturchio, N. C.; Grace, J. D.; Geissbuhler, P.; Sorensen, L. B.; Cheng, L.; Xu, S. *Geochim. Cosmochim. Acta* **1997**, *61*, 1467.

(36) Sturchio, N. C.; Chiarello, R. P.; Cheng, L.; *Geochim. Cosmochim. Acta* **1997**, *61*, 251.

(37) Little, L. H. *Infrared Spectra of Adsorbed Species*; Academic Press: London, 1966.

(38) Hair, M. L. *Infrared Spectroscopy in Surface Chemistry*; Marcel Dekker: New York, 1967.

(39) Anderson, P. J.; Horlock, R. F.; Oliver, J. F. *Trans. Faraday Soc.* **1965**, *61*, 2754.

(40) Gallei, E.; Parks, G. A. *J. Colloid. Interface Sci.* **1972**, *38*, 650.

(41) Tsyganenko, A. A.; Filimonov, V. N. *J. Mol. Struct.* **1973**, *19*, 579.

(42) Parfitt, R. L.; Russell, J. D.; Farmer, V. C. *J. Chem. Soc., Faraday Trans. 1* **1976**, *72*, 1082.

(43) Koretsky, C. M.; Sverjensky, D. A.; Salisbury, J. W.; D'Aria, D. M. *Geochim. Cosmochim. Acta* **1997**, *61*, 2193.

(44) Gård, R.; Sun, Z.; Forsling, W. *J. Colloid Interface Sci.* **1995**, *169*, 393.

(45) Tejedor-Tejedor, I. M.; Anderson, M. *Langmuir* **1986**, *2*, 203–210.

(46) Zeltner, W. A.; Anderson, M. A. *Langmuir* **1988**, *4*, 469.

(47) Tejedor-Tejedor, M. I.; Anderson, M. A. *Langmuir* **1990**, *6*, 602.

(48) Persson, P.; Nilsson, N.; Sjöberg, S. *J. Colloid. Interface Sci.* **1996**, *177*, 263.

(49) Persson, P.; Lövgren, L. *Geochim. Cosmochim. Acta* **1996**, *60*, 2789.

(50) Hug, S. J. *J. Colloid. Interface Sci.* **1997**, *188*, 415.

(51) Eggleston, C. M.; Hug, S.; Stumm, W.; Sulzberger, B.; Dos Santos A. M. *Geochim. Cosmochim. Acta* **1998**, *62*, 585.

(52) Rao, H. K.; Cases, J. M.; De Donato, P.; Forssberg, K. S. E. *J. Colloid Interface Sci.* **1991**, *145*, 314.

(53) Mielczarski, J. A.; Cases, J. M.; Bouquet, E.; Barres, O.; Delon, J. F. *Langmuir* **1993**, *9*, 2370.

(54) Mielczarski, J. A.; Cases, J. M.; Tekely, P.; Canet, D. *Langmuir* **1993**, *9*, 3357.

(55) Mielczarski, J. A.; Mielczarski, E. *J. Phys. Chem.* **1995**, *99*, 3206.

(56) Mielczarski, J. A.; Cases, J. M. *Langmuir* **1995**, *11*, 3275.

(57) Mielczarski, E.; Mielczarski, J. A. *Langmuir* **1998**, *14*, 1739.

(58) Charlet, L.; Wersin, P.; Stumm, W. *Geochim. Cosmochim. Acta* **1990**, *54*, 2329.

(59) Pokrovsky, O. S.; Schott, J.; Thomas, F. *Geochim. Cosmochim. Acta* **1999**, *63*, 863.

(60) Van Cappellen, P.; Charlet, L.; Stumm, W.; Wersin, P. *Geochim. Cosmochim. Acta* **1993**, *57*, 3505.

(61) Pokrovsky, O. S.; Schott, J.; Thomas, F. *Geochim. Cosmochim. Acta* **1999**, *63* (19/20).

(62) Arakaki, T.; Mucci, A. *Aquatic Geochemistry* **1995**, *1*, 105.

(63) Sternbeck, J. *Geochim. Cosmochim. Acta* **1997**, *61*, 785.

(64) Nilsson, Ö.; Sternbeck, J. *Geochim. Cosmochim. Acta* **1999**, *63*, 217.

(65) Pokrovsky, O. S.; Schott, J. *Geochim. Cosmochim. Acta* **1999**, *63*, 881.

(66) Schindler, P. W.; Stumm, W. In *Aquatic Surface Chemistry*; Stumm, W., Ed.; J. Wiley & Sons: New York, 1987; p 83.



**Table 1. Composition of Investigated Solutions for Calcite Samples**

#	solution	<i>I</i> , M	[Alk], M	[Ca <sup>2+</sup> ] <sub>tot</sub> , M	pH
C1	0.1 M NaCl+HCl	0.10	$4 \times 10^{-4}$	0.01	$5.2 \pm 0.2$
C2	0.1 M NaCl+HCl	0.10	0.004 25	0.004	$6.2 \pm 0.2$
C3	0.03 M NaCl+HCl	0.03	0.002 58	0.0044	$5.9 \pm 0.2$
C4	0.05 M NaCl+HCl	0.05	0.002 50	0.0219	$6.3 \pm 0.2$
C5	0.01 M NaHCO <sub>3</sub>	0.01	0.010	$7.5 \times 10^{-5}$	$8.58 \pm 0.02$
C6	0.01 M Na <sub>2</sub> CO <sub>3</sub>	0.03	0.019	$1.0 \times 10^{-5}$	$10.90 \pm 0.01$
C7	0.1 M NaHCO <sub>3</sub>	0.10	0.0968	$2.6 \times 10^{-5}$	$8.52 \pm 0.01$
C8	0.01 M NaOH	0.01	0.0108	$2.93 \times 10^{-5}$	$11.96 \pm 0.01$

surface hydroxyl and carbonate groups determined from the infrared reflection spectra of calcite and dolomite samples exposed to different aqueous solutions with the concentration of surface species predicted from the surface complexation models for these two minerals.

### Materials and Methods

**Solid Phases.** Natural pure dolomite and calcite were purchased from Ward's Natural Science Establishment, Inc. Chemical analysis of these minerals performed by ICP-MS showed only trace amounts (<0.1%) for all investigated impurities (Cd, Zn, Cu, Pb, Mn, Co, Ni, Fe, Ba, Sr, As, Se, Y, REE). The samples were ground in an agate mortar to a powder of <10  $\mu$ m. This provides surface areas of 2.8 m<sup>2</sup>/g and 1.7 m<sup>2</sup>/g for dolomite and calcite, respectively, as determined by N<sub>2</sub> BET absorption. A small particle size is required to avoid unwanted optical effects which complicate the interpretation of reflection spectra. Besides, an increase in the surface area greatly increases the amount of surface species and provides faster equilibration of the powder with aqueous solution.

**Samples Preparation.** Stock solutions of NaHCO<sub>3</sub>, Na<sub>2</sub>CO<sub>3</sub>, NaCl, HCl, and NaOH were made from Prolabo reagent grade salts and from Merck (Titrisol) standard solutions, using deionized (18 M $\Omega$ ) water. To prepare a suspension of the solid phase, 0.3 g of mineral powder was placed in a 30-mL plastic vial with solution containing a known amount of carbonate. The pH of the solution was adjusted to the required value. This suspension was allowed to preequilibrate for 1–2 days at room temperature. The solutions were kept open to the atmosphere during preequilibration. For samples prepared at pH < 6 only a short preequilibration time (1–5 min) was possible due to fast neutralization of solutions. These conditions lead to the achievement of an equilibrium distribution of the surface species although the equilibrium with the bulk solid is not necessarily fulfilled. This implies that all surface reactions leading to the formation of surface complexes should be very fast compared to the bulk solid dissolution/precipitation processes, an assumption which is frequently used for short-term surface titration studies.<sup>58</sup>

Immediately after powder sampling the solution pH was measured and the supernatant was filtered for analysis of alkalinity ([Alk] = [HCO<sub>3</sub><sup>-</sup>] + 2[CO<sub>3</sub><sup>2-</sup>] + [OH<sup>-</sup>]) and total dissolved metal concentration ([Me<sup>2+</sup>]<sub>tot</sub>). For samples having pH < 7, continuous monitoring of pH as a function of time in the remaining suspension was performed. During 1 h of reaction, the associated uncertainties never exceeded 0.2 pH units. Solution compositions are presented in Tables 1 and 2 for the experiments performed with calcite and dolomite, respectively. The solution pH varied from 3 to 12, [Alk] and [Me<sup>2+</sup>]<sub>tot</sub> ranged from 10<sup>-5</sup> to 0.1 M and from 10<sup>-5</sup> to 0.02 M, respectively, and ionic strength (*I*) varied from 0.01 to 0.1 M. The pH was measured with an uncertainty of 0.1 units in neutral to acid solutions and 0.01 units in alkaline solutions. [Alk] was measured following a standard procedure of HCl titration with an uncertainty of 1%. Total dissolved calcium and magnesium were measured by flame atomic absorption spectroscopy with an uncertainty of 1%.

**Infrared Analysis.** The diffuse reflectance (DRIFT) spectra were recorded on a Bruker IFS55 FTIR spectrometer with an MCT detector by means of a diffuse reflectance attachment. The accessory was from Harrick Scientific Co. The spectrometer was purged with CO<sub>2</sub>-free dry air (Balston Filter). A sample of the powder was separated from solution by decantation and put on filter paper to remove excess solution. 50 mg of such semidry powder was dispersed in 350 mg of KBr and lightly packed into

a 10 mm diameter microsampling cup. The spectra were taken at 4 cm<sup>-1</sup> resolution by coadding up to 200 scans in the 4000–500 cm<sup>-1</sup> region. The unit of intensity was defined as  $-\log(R/R_0)$  where  $R_0$  and  $R$  are the reflectivities of the system without and with the investigated medium, respectively. Atmospheric water was always subtracted. The intensities of the absorbance bands were measured from the tangentially drawn baselines.

All spectra were measured as a function of residence time in the spectrophotometer chamber (at the beginning every 2 min), in which the mineral samples were held at about 25 °C. The reflection spectra of the different mineral samples prepared in the same solution conditions were recorded showing very good reproducibility of the produced surface composition in the independent experiments.

### Results and Discussion

**Surface Speciation Calculations.** The surface complexation models (SCMs) of dolomite<sup>61</sup> and calcite<sup>60,61</sup> were used in this study. In the context of SCM, all surface reactions are written explicitly in terms of the two primary hydration sites, >MeOH<sup>o</sup> and >CO<sub>3</sub>H<sup>o</sup>. It is proposed that the hydration of the fresh mineral surface leads to the formation of the following surface species: >MeOH<sub>2</sub><sup>+</sup>, >MeOH<sup>o</sup>, >MeO<sup>-</sup>, >MeHCO<sub>3</sub><sup>o</sup>, >MeCO<sub>3</sub><sup>-</sup>, >CO<sub>3</sub>Me<sup>+</sup>, >CO<sub>3</sub>H<sup>o</sup>, and >CO<sub>3</sub><sup>-</sup>. The surface reactions and their intrinsic stability constants ( $K^o_{int}$ ) are listed in Table 3. In the present study, the surface densities of each site were designed as 8 and 14  $\mu$ mol/m<sup>2</sup> for calcite and dolomite, respectively. This corresponds to 5 and 8 sites per nm<sup>2</sup> originating from crystallographic data for {1014} cleavage planes and is based also on the surface charge data.<sup>60,61</sup> A constant capacitance model of the electric double layer with the capacitance of  $I^{1/2}/0.006$  (F/m<sup>2</sup>) for calcite and  $I^{1/2}/0.004$  (F/m<sup>2</sup>) for dolomite, where  $I$  (M) is ionic strength, was used. The surface stability constants for calcite were proposed based on the analogy between homogeneous reactions in solution and the corresponding reactions on the surface.<sup>60,66</sup> This set of surface stability constants was found to satisfy the conditions of zero charge of calcite at pH 8.2 in equilibrium with atmosphere as determined by electrokinetic measurements.<sup>67</sup> We attempted further refinement of calcite SCM<sup>60</sup> based on the relationships between the isoelectric point and solution composition obtained by electrophoresis and streaming potential techniques in a wide range of solution pH.<sup>1–3,25,66–72</sup> As a result, values of  $K^o_{int}$  for surface reactions on calcite were derived (Table 3). Note that this set of surface stability constants determined with an uncertainty of 0.3 log units presents a first-order description amenable to further refinement.

For dolomite, only a limited amount of literature data on electrokinetics is available (see ref 73 and references therein). A detailed study of the dolomite/water interface was performed<sup>61</sup> in which streaming potential, electrophoresis, and surface titration techniques were combined to characterize the surface charge of dolomite and its dependence on solution composition. Based on these data, a surface complexation model of dolomite was proposed with the unique set of surface stability constants listed

(67) Mishra, S. K. *Int. J. Miner. Process.* **1978**, *5*, 69.

(68) Douglas, H. W.; Walker, R. A. *Trans. Faraday Soc.* **1950**, *46*, 559.

(69) Somasundaran, P.; Agar, G. E. *J. Colloid Interface Sci.* **1967**, *24*, 433.

(70) Fuerstenau, M. C.; Gutierrez, G.; Elgillani, D. A. *Trans. AIME* **1968**, *241*, 319.

(71) Foxall, T.; Peterson, G. C.; Rendall, H. M.; Smith, A. L. *J. Chem. Soc., Faraday Trans 1* **1979**, *75*, 1034.

(72) Amankonah, J. O.; Somasundaran, P. *Colloids Surf.* **1985**, *15*, 335.

(73) Predali, J.-J.; Cases, J.-M. *J. Coll. Interface Sci.* **1973**, *45*, 449.

**Table 2. Composition of Investigated Solutions for Dolomite Samples**

#	solution	<i>I</i> , M	[Alk], M	[Ca <sup>2+</sup> ] <sub>tot</sub> , M	[Mg <sup>2+</sup> ] <sub>tot</sub> , M	pH
D1	0.1 M NaCl+HCl	0.10	0.0	0.021	0.022	3.0 ± 0.2
D2	0.1 M NaCl+HCl	0.10	1 × 10 <sup>-4</sup>	0.0105	0.0108	5.0 ± 0.1
D3	0.1 M NaCl+HCl	0.10	0.0	0.0210	0.0205	5.3 ± 0.1
D4	0.1 M NaCl+HCl	0.10	0.0010	0.0150	0.014	5.4 ± 0.1
D5	0.09 M NaCl+HCl	0.09	0.0014	0.0154	0.0137	5.5 ± 0.1
D6	0.08 M NaCl+HCl	0.08	0.0029	0.0144	0.0124	6.6 ± 0.1
D7	0.01 M NaCl+HCl	0.01	0.0032	0.003 05	0.003 09	6.56 ± 0.05
D8	0.01 M NaHCO <sub>3</sub>	0.01	0.0080	1.84 × 10 <sup>-4</sup>	3.07 × 10 <sup>-4</sup>	7.10 ± 0.05
D9	0.01 M NaCl	0.01	0.0046	0.001 27	0.0016	7.75 ± 0.05
D10	0.01 M NaHCO <sub>3</sub>	0.01	0.0106	1.34 × 10 <sup>-4</sup>	2.87 × 10 <sup>-4</sup>	8.72 ± 0.02
D11	0.009 M NaCl	0.01	0.002 26	4.76 × 10 <sup>-4</sup>	4.95 × 10 <sup>-4</sup>	8.78 ± 0.02
D12	0.01 M NaCl	0.01	0.004 90	1.80 × 10 <sup>-4</sup>	2.30 × 10 <sup>-4</sup>	8.52 ± 0.02
D13	0.01 M NaHCO <sub>3</sub>	0.01	0.009 28	0.00118	6.73 × 10 <sup>-4</sup>	7.28 ± 0.02
D14	0.01 M Na <sub>2</sub> CO <sub>3</sub>	0.03	0.02	2.3 × 10 <sup>-5</sup>	3.1 × 10 <sup>-5</sup>	10.73 ± 0.01
D15	0.1 M NaHCO <sub>3</sub>	0.10	0.0964	4.48 × 10 <sup>-4</sup>	1.16 × 10 <sup>-4</sup>	8.74 ± 0.01
D16	0.1 M Na <sub>2</sub> CO <sub>3</sub>	0.30	0.20	1.8 × 10 <sup>-5</sup>	2.8 × 10 <sup>-5</sup>	11.30 ± 0.01
D17	0.01 M NaOH	0.01	0.008 85	3.28 × 10 <sup>-5</sup>	2.56 × 10 <sup>-5</sup>	11.71 ± 0.01
D18	0.01 M MgCl <sub>2</sub>	0.03	0.0011	1.2 × 10 <sup>-4</sup>	0.01	8.90 ± 0.02
D19	0.05 M MgCl <sub>2</sub>	0.15	8.0 × 10 <sup>-4</sup>	1.8 × 10 <sup>-4</sup>	0.05	9.10 ± 0.05
D20	0.1 M MgCl <sub>2</sub>	0.3	0.0030	1.5 × 10 <sup>-5</sup>	0.10	8.90 ± 0.05
D21	0.05 M CaCl <sub>2</sub>	0.15	5.1 × 10 <sup>-4</sup>	0.05	6.1 × 10 <sup>-4</sup>	8.70 ± 0.05
D22	0.1 M CaCl <sub>2</sub>	0.30	2.2 × 10 <sup>-4</sup>	0.10	1.1 × 10 <sup>-4</sup>	8.50 ± 0.05

**Table 3. Surface Complexation Reactions and Their Intrinsic Stability Constants (K<sup>o</sup><sub>int</sub>) at the Calcite and Dolomite/Solution Interface**

reaction on the surface	log K <sup>o</sup> <sub>int</sub> (25 °C, <i>I</i> = 0)		
	calcite (Ca)	dolomite	
		(Ca)	(Mg)
1. >CO <sub>3</sub> H <sup>o</sup> = >CO <sub>3</sub> <sup>-</sup> + H <sup>+</sup>	-5.1	-4.8 ± 0.2	-4.8 ± 0.2
2. >CO <sub>3</sub> H <sup>o</sup> + Me <sup>2+</sup> = >CO <sub>3</sub> Me <sup>+</sup> + H <sup>+</sup>	-1.7	-1.8 ± 0.2	-2.0 ± 0.2
3. >MeOH <sup>o</sup> - H <sup>+</sup> = >MeO <sup>-</sup>	-12	-12 ± 2	-12 ± 2
4. >MeOH <sup>o</sup> + H <sup>+</sup> = >MeOH <sub>2</sub> <sup>+</sup>	11.5	11.5 ± 0.2	10.6 ± 0.2
5. >MeOH <sup>o</sup> + CO <sub>3</sub> <sup>2-</sup> + 2H <sup>+</sup> = >MeHCO <sub>3</sub> <sup>o</sup> + H <sub>2</sub> O	23.5	24.0 ± 0.5	23.5 ± 0.5
6. >MeOH <sup>o</sup> + CO <sub>3</sub> <sup>2-</sup> + H <sup>+</sup> = >MeCO <sub>3</sub> <sup>-</sup> + H <sub>2</sub> O	17.1	16.6 ± 0.2	15.4 ± 0.2

in Table 3. Note that the constants of surface reactions for dolomite may be determined with much lower uncertainties than those for calcite due to the large amount of data on the surface charge collected by surface titration and electrokinetic techniques in a wide range of solution composition. The accepted set of surface stability constants for calcite and dolomite was used to calculate the surface speciation of both minerals in different aqueous solutions whose compositions are presented in Tables 1 and 2. This calculation was performed by means of MINTEQA2 computer code<sup>74</sup> which uses the principle of mass and charge balance conditions for a given solution composition (pH, [Alk], [Me<sup>2+</sup>]<sub>tot</sub>). The detailed description of this procedure is given elsewhere.<sup>60,74</sup> The MINTEQA2 program was also used to calculate the equilibrium species distribution in the CaO–MgO–CO<sub>2</sub>–H<sub>2</sub>O homogeneous solution system. The activity coefficients of aqueous ions were calculated using the Davies equation. The equilibrium constants used in the solution speciation calculation at 25 °C were taken from the MINTEQA2 database.<sup>75</sup>

Examples of surface speciation calculations for the dolomite and calcite/water interfaces in 0.01 M NaCl solutions in equilibrium with atmospheric CO<sub>2</sub> are shown in Figure 1. As it is seen from this figure, the dominant surface species on the metal sites are >MeOH<sub>2</sub><sup>+</sup> and >MeCO<sub>3</sub><sup>-</sup>. In the neutral to alkaline pH range, the carbonate sites are always represented by >CO<sub>3</sub><sup>-</sup> species

whereas at pH 6 for calcite and 8 for dolomite, the >CO<sub>3</sub>H<sup>o</sup> species becomes dominant. In contrast, the metal sites are represented by >MeOH<sub>2</sub><sup>+</sup> species at pH 8. With increasing pH and CO<sub>2</sub> levels, >MeCO<sub>3</sub><sup>-</sup> becomes dominant. Note that the speciation at metal sites is very sensitive to the total aqueous carbonate concentration in solution. For illustration, the mole fraction of >MeOH<sub>2</sub><sup>+</sup> groups of mineral surfaces exposed to solutions having different carbonate concentrations is shown as a function of pH for calcite (Figure 2A) and dolomite (Figure 2B). For both minerals, the >MeOH<sub>2</sub><sup>+</sup> concentration decreases dramatically with increasing pH and aqueous carbonate concentration as these species are replaced by adsorbed carbonate, >MeCO<sub>3</sub><sup>-</sup>. Thus, it is anticipated that varying pH and CO<sub>2</sub> content in solution should allow us to change the surface concentration of the OH and CO<sub>3</sub> groups. Such major changes in surface composition should be detectable by IR spectroscopy.

**Basis of Infrared Studies of the Surface Hydroxyl and Carbonate Groups on Calcite and Dolomite.** The optical properties of calcite and dolomite in the infrared region have been summarized by White.<sup>76</sup> There are three strong bands in the mid-infrared region (Figures 3 and 4) which are due to the internal modes of the CO<sub>3</sub><sup>2-</sup> ion, and assigned to three infrared active fundamental vibrations:  $\nu_4$  in-plane bending,  $\nu_2$  out-of-plane bending, and  $\nu_3$  asymmetric stretching at about 700, 900, and 1400–1500 cm<sup>-1</sup>, respectively. The latter vibration shows a very broad band which results from very large splitting of the transverse and longitudinal components of the vibration. The magnitude of the splitting is related to the absorption

(74) Allison, J. D.; Brown, D. S.; Novo-Gradac, K. J. *MINTEQA2/PRODEFA2, A geochemical assessment model for environmental systems: version 3.0 user's manual*; U. S. EPA, Athens, GA, 1991.

(75) Nordstrom, D. K.; Plummer, N. L.; Langmuir, D.; Busenberg, E.; May, H. M.; Jones, B. F.; Parkhurst, D. L. In *Chemical Modeling of Aqueous Systems II*; Melchior, D. C., Bassett, R. L., Eds.; ACS Symp. Ser., 1990; p 398.

(76) White, W. B. In *The Infrared Spectra of Minerals*; Farmer, V. C., Ed.; Mineral. Soc. London, 1974; p 87.

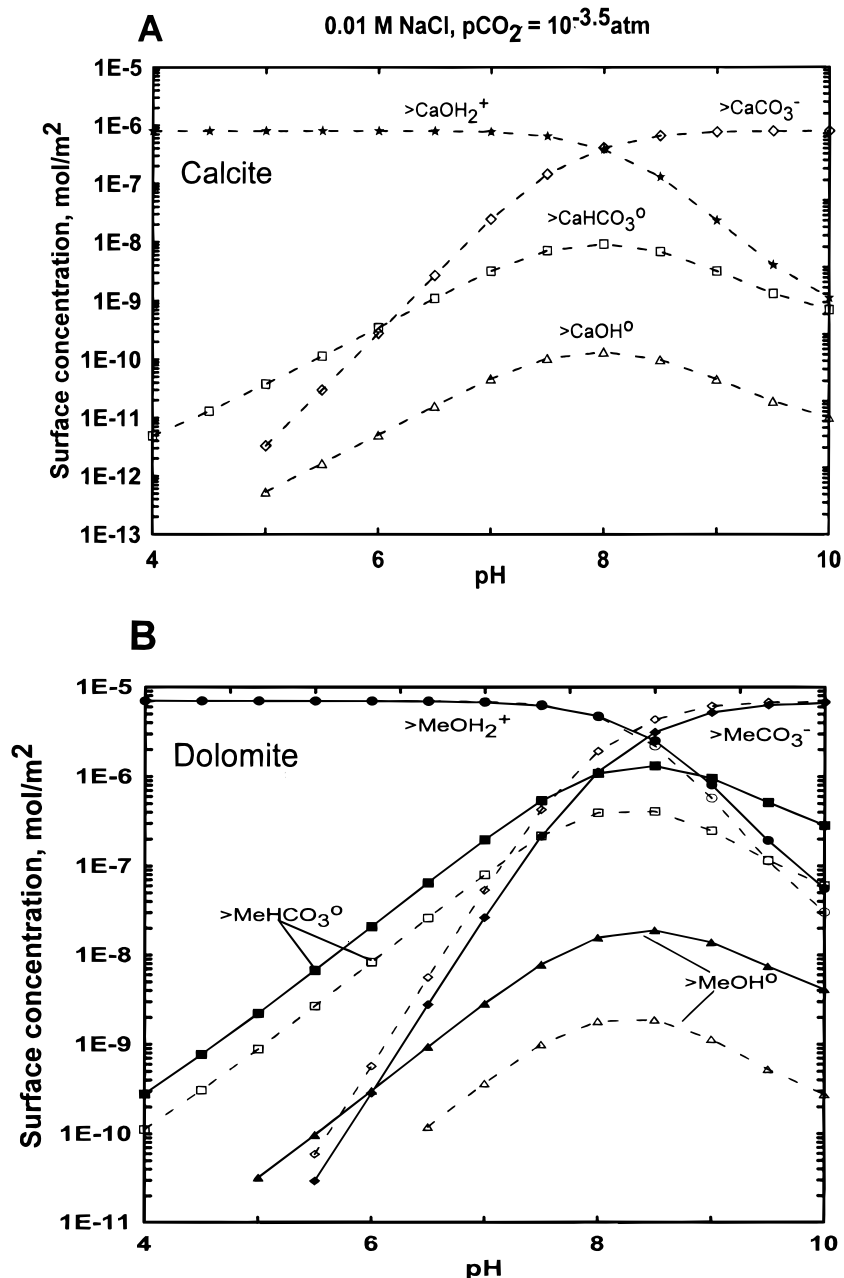


**Figure 1.** Calculated speciation at the metal sites of calcite (A) and dolomite (B)/water interface at 25 °C,  $I = 0.01$  M,  $[\text{Me}^{2+}]_{\text{tot}} = 10^{-3}$  M, and  $p\text{CO}_2 = 10^{-3.5}$  atm. Mg, solid lines and closed symbols; Ca, dashed lines and open symbols.

strength which is very high for both minerals. Similar positions of the absorbance bands can be found for calcite and dolomite (Figures 3 and 4). Transmission spectra of both carbonates exhibit a large number of low intensity bands in the region of frequency up to  $4000\text{ cm}^{-1}$  which are assigned to a combination of the internal and lattice modes. Though these bands at about  $1800$ ,  $2500$ , and  $2900\text{ cm}^{-1}$  show relatively high intensities compared with the fundamental vibrations (the bands at about  $1400$ ,  $900$ , and  $700\text{ cm}^{-1}$ ) in the spectra recorded in the diffuse reflectance mode (which is a common effect) they will not be applied in this study because of the complexity of the vibrations.

The strong carbonate fundamental absorbance bands make monitoring of any characteristic bands of the surface species in their frequency region difficult. It is very arduous to determine the type and density of surface carbonate groups such as  $>\text{MeCO}_3^-$ ,  $>\text{MeHCO}_3^0$ ,  $>\text{CO}_3^-$ ,  $>\text{CO}_3\text{H}^0$ , whose absorbance bands appear at the same region of

frequency as the absorbance bands of the bulk carbonate groups. The characterization of the surface  $>\text{MeOH}_2^+$ ,  $>\text{MeOH}^0$  groups is also difficult. An in situ investigation of the surface groups, which would be the most correct experimental way for the determination of the surface species produced in aqueous solution, is practically impossible because of full overlapping of the stretching (the broad bands at about  $3400\text{ cm}^{-1}$ ) and bending (the band at about  $1600\text{ cm}^{-1}$ ) absorbance bands of the OH surface groups with those of water showing absorbance in the same region. Therefore, to obtain plausible information about the surface carbonate and hydroxyl groups formed on calcite and dolomite in aqueous solutions of different composition, the reflection spectra were measured as a function of residence time in spectrophotometric chamber. Each of the first recorded infrared spectra of the mineral sample shows a very broad absorbance band at about  $3400\text{ cm}^{-1}$  (Figures 3a and 4a) indicating the presence of a significant amount of water in the inves-



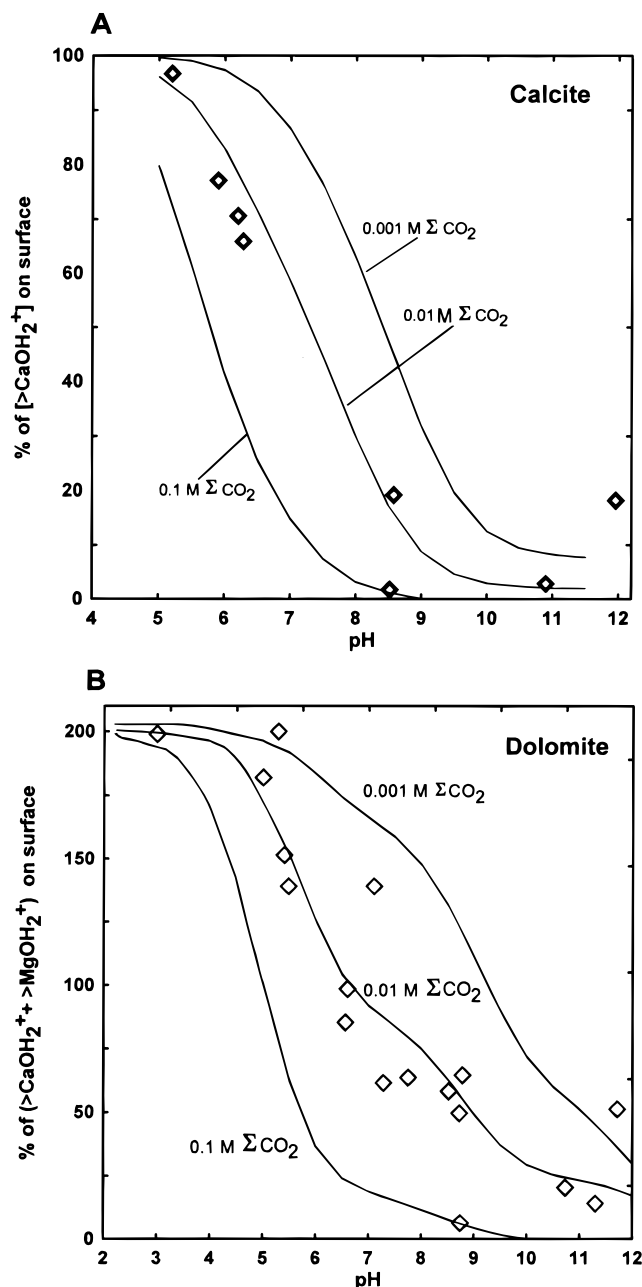


**Figure 2.** Relative surface concentration of  $>\text{MeOH}_2^+$  species (% from  $8 \mu\text{mol}/\text{m}^2$ ) as a function of pH in solutions having different carbonate concentration for calcite (A) and dolomite (B) calculated by complexation model. The symbols represent the experimental points from Tables 1 and 2.

tigated sample. The intensity of the band sharply decreases after a few minutes of holding in the spectrophotometer chamber (spectra were recorded every 2 min), and then stabilizes showing almost the same spectral feature in the spectra recorded during the next 20 min of the spectroscopic investigation (Figures 3c,d and 4c,e). This procedure allows us to make the reasonable assumption that the first unaltered reflection spectra (obtained after a quick removal of the liquid and physisorbed water as illustrated by the lowering of the  $3400 \text{ cm}^{-1}$  band) carry the most information about the surface species produced in different solution conditions. Thus, the spectra recorded within the first 10–30 min holding of the sample in spectrophotometer chamber were used for SCM evaluation in this study. A prolongation of the holding of the sample in the spectrophotometer chamber causes slow continuous

changes in the surface compositions (Figure 4e and 4f). For example, after 3 days in the spectrophotometer a significant increase of density of the carbonate surface groups is observed as demonstrated by the difference spectrum in Figure 4g whereas the density of the surface hydroxyl groups remains practically the same. Note that such changes in surface composition were negligible during 1 h of holding in the spectrophotometer as illustrated in Figure 4h.

**Monitoring of Surface Hydroxyl and Carbonate Groups.** An example of infrared spectra recorded for dolomite which was in contact with different solutions is presented in Figure 5. The spectra of these samples show significant differences in the fundamental bands of the carbonate and hydroxyl groups which are related to the nature of the species present at the mineral surface. The difference spectrum of the samples treated in acid and basic solutions (Figure 5c) shows very interesting features. It can be concluded that dolomite treated in acidic solution has a higher density of surface hydroxyl groups, the positive bands at  $3421$ ,  $3237$ , and  $1631 \text{ cm}^{-1}$ , and less surface carbonate groups, the negative bands of fundamental vibrations at  $1494$ ,  $1430$ ,  $883$ , and  $728$ , and their low intensity satellites at  $854$  and  $713 \text{ cm}^{-1}$ .

It is not possible to have a perfect reference spectrum of dolomite without any surface adsorption groups; therefore, the changes in the relative intensity of the characteristic hydroxyl and carbonate absorbance bands in the spectra of samples prepared in different solutions will be used in the study. It is noteworthy that the surface carbonates show the positions of the absorbance bands shifted to higher frequency for  $\nu_2$  and  $\nu_3$  modes indicating a good possibility to distinguish the surface carbonate species from the bulk carbonate groups. The presence of two bands at  $1494$  and  $1430 \text{ cm}^{-1}$  for the surface carbonate species (Figure 5c) could be caused by the splitting of the transverse and longitudinal components of the vibration, similar to that of the bulk signal. Because the splitting is much stronger than that for the bulk signal it could also reflect the presence of different types of surface carbonate species, (i.e.,  $>\text{MeCO}_3^-$ ,  $>\text{MeHCO}_3^0$ ). The absorbance bands assigned to the hydroxyl surface group also indicate the presence of two different surface species with bands at  $3421$  and  $3237 \text{ cm}^{-1}$ . It should be noted that the low intensity sharp bands at  $3176$ ,  $3216$ , and  $3583 \text{ cm}^{-1}$  for calcite (Figure 6), and the bands at  $3180$ ,  $3237$ , and  $3608 \text{ cm}^{-1}$  for dolomite (Figure 5) are assigned to the combination bands of carbonate groups. In the case of calcite the difference spectrum of the samples prepared in acid and basic solutions (Figure 6c) shows an increase of the density of the surface hydroxyl groups with a coincident decrease in density of the carbonate groups. This is similar to that found for dolomite (Figure 5c).

This discussion demonstrates a real possibility to distinguish between different species formed on calcite and dolomite surfaces, especially if additional experimental results are available. However, in this work only changes of the total integrated intensity of the hydroxyl groups (the bands about  $3400 \text{ cm}^{-1}$ ) and carbonate groups (the broad bands at about  $1450 \text{ cm}^{-1}$ ) will be discussed without a detailed specification of the type of the surface hydroxyl ( $>\text{CaOH}_2^+$ ,  $>\text{MgOH}_2^+$ ) and carbonate ( $>\text{MeCO}_3^-$ ,  $>\text{MeHCO}_3^0$ ) groups.

The measured integrated intensity of OH bands at about  $3400 \text{ cm}^{-1}$  correlates well with the predicted concentration of OH groups at the calcite or dolomite surface for all the investigated samples in a very broad range of solution composition (Figures 7 and 8, respectively). These results indicate that the  $>\text{MeOH}_2^+$  surface species are responsible

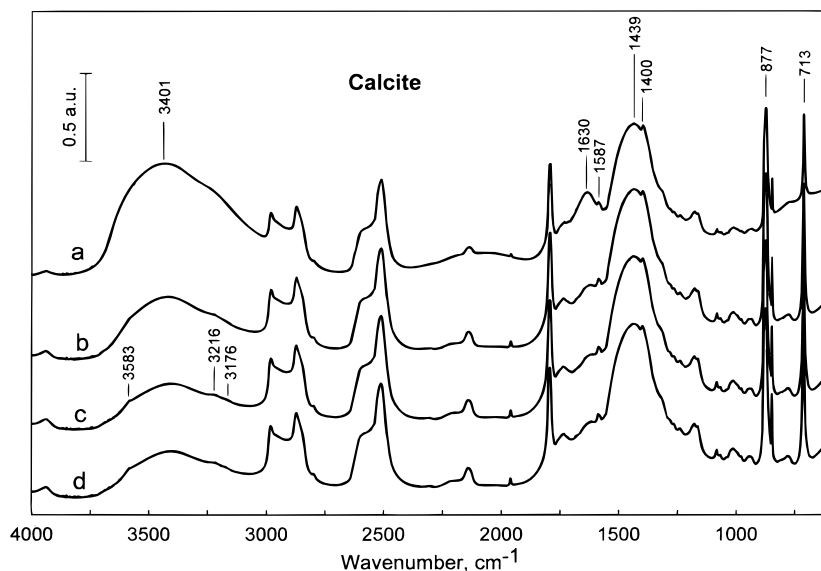


**Figure 3.** DRIFT spectra of calcite sample (C1) after contact with aqueous solution at pH = 5.2. (a): wet sample; (b), (c), and (d): after 10, 20, and 30 min drying in spectrophotometer.

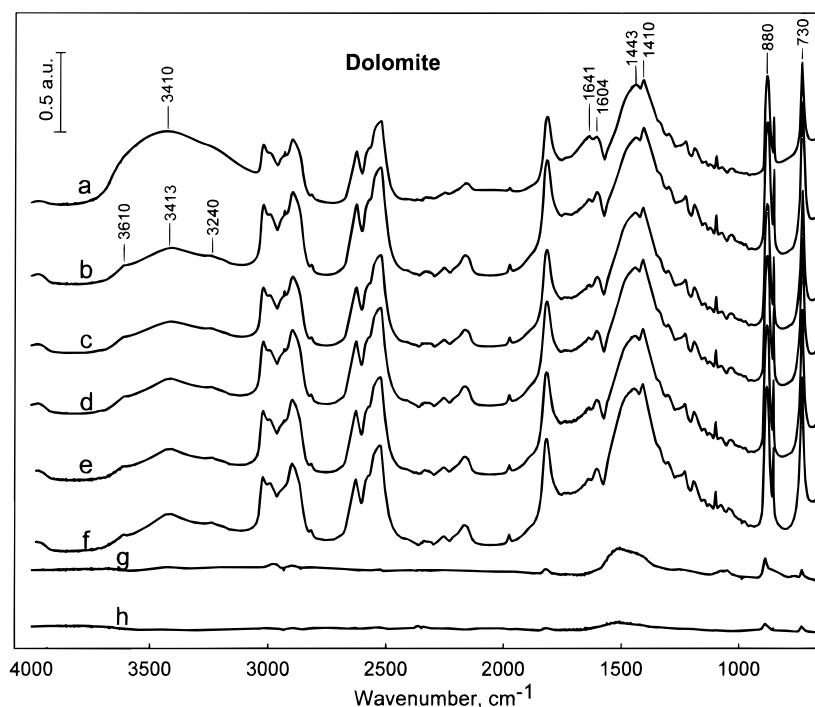


**Figure 4.** DRIFT spectra of dolomite sample D5 (pH = 5.5) as a function of residence time in the spectrometer. (a): wet sample; (b), (c), (d), (e), and (f): after 10, 20, 30, 60 min, and 3 days in the spectrometer; (g): difference spectrum of 3 days (f)–30 min (d); (h): difference spectrum of 60 min (e)–30 min (d).

for the observed stretching absorbance bands. It should be noted that the intensity of the OH bending bands at  $1635\text{ cm}^{-1}$  also increases with decreasing pH (Figure 9).

At pH from 3 to 9, significant changes in the shape of double carbonate and hydroxyl bands at  $1408\text{ cm}^{-1}$  and hydroxyl bands at  $3405$  and  $1635\text{ cm}^{-1}$  were observed (Figure 9). These changes may be attributed to the formation of the  $>\text{MeCO}_3^-$  and  $>\text{MeHCO}_3^0$  surface species which dominate at the dolomite surface at pH above 8.5 according to SCM calculations (Figure 1).

To illustrate the adsorption of the OH and  $\text{CO}_3$  groups from solution on mineral surfaces, the measured band intensities ratio  $[\text{OH}]_{\text{total}}/[\text{CO}_3]_{\text{total}} = I_{3265-3550\text{ cm}^{-1}}/I_{1052-1573\text{ cm}^{-1}}$  has been plotted as a function of

the predicted surface concentration ratio  $\{>\text{MeOH}_2^+\}/\{>\text{MeHCO}_3^0 + >\text{MeCO}_3^-\}$ . This ratio is not affected by a possible experimental error associated with sample preparations for spectroscopic study. Figure 10 shows results from all experimental data described in Tables 1 and 2 and the related simulated values. Taking into account all the difficulties, already discussed in this work, of the experimental determination of the OH and  $\text{CO}_3$  group surface densities, the relationships presented in Figure 10 for calcite and dolomite are considered to have very good agreement between the experimental and simulated data. It is interesting to note that the highest points which represent data at most acidic solutions (the conditions of the mineral significant dissolution) are also in line with predicted values.



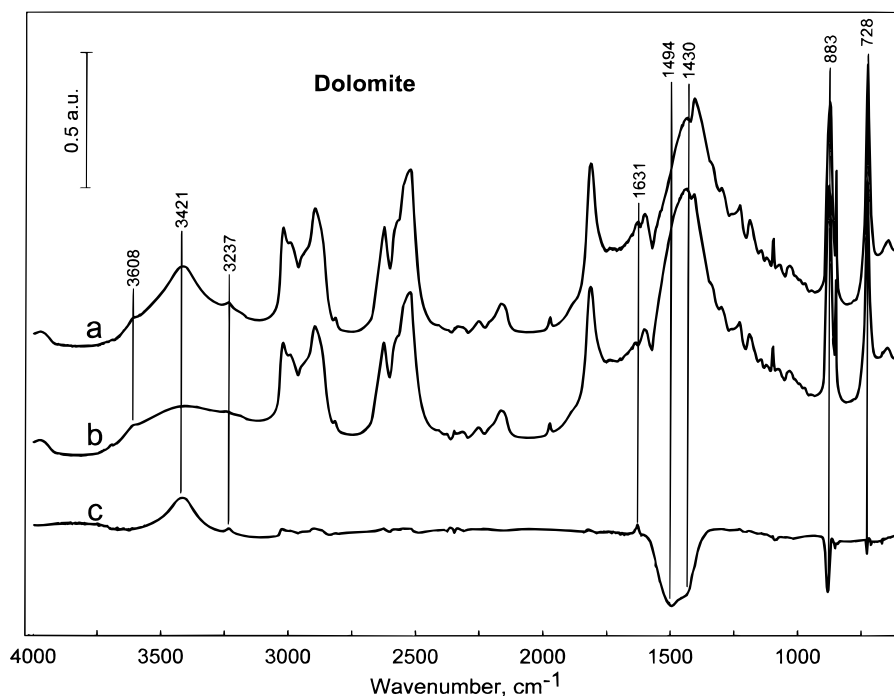


**Figure 5.** DRIFT spectra of dolomite samples after contact with different solutions: (a) D3, pH = 5.3; (b) D11, pH = 8.8; (c) difference spectrum of (D3)–(D11).

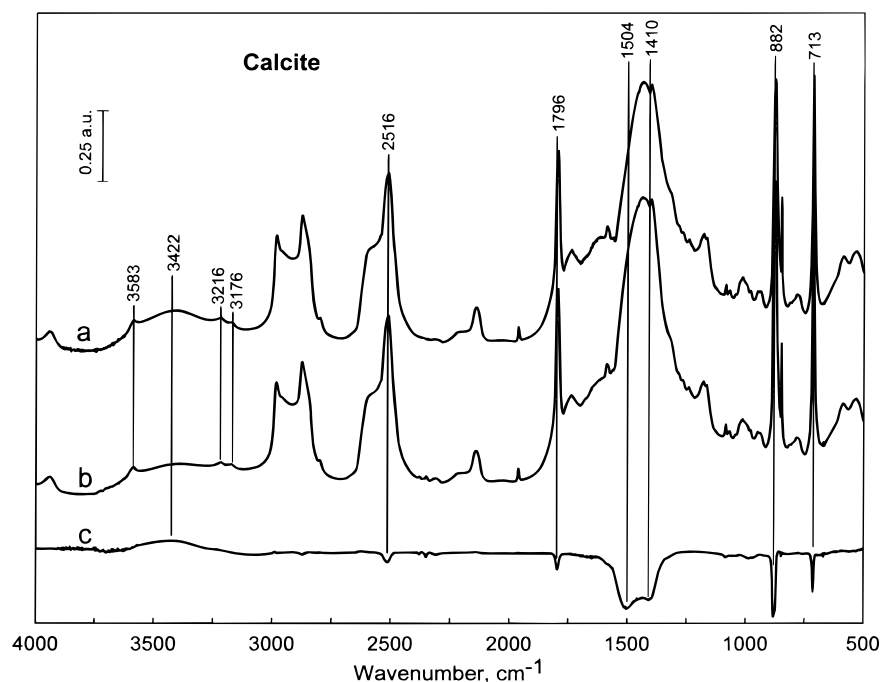


**Figure 6.** DRIFT spectra of calcite samples after contact with different solutions: (a) C4, pH 6.3; (b) C6, pH 10.9; (c) difference spectrum of (C4)–(C6).

The demonstrated relationships between the predicted and experimentally determined densities of the hydroxyl and carbonate type groups on the calcite and dolomite surface indicates a consistency between the results of IR-surface characterization and the surface speciation modeling.

**Influence of the Addition of Calcium and Magnesium Ions on Dolomite Surface Composition.** An additional set of experiments was performed to characterize the form of adsorbed Ca and Mg onto the dolomite surface. Within the context of SCM, adsorption of these ions leads to the formation of  $>\text{CO}_3\text{Ca}^+$  and  $>\text{CO}_3\text{Mg}^+$  surface species. These species, however, may contain water

in their first hydration sphere ( $>\text{CO}_3\text{Me}^+ \times n\text{H}_2\text{O}$ ) which should give rise to the absorbance of the OH stretching vibration at about  $3400\text{ cm}^{-1}$  in the spectra associated with adsorbed metal. In this regard, the  $>\text{CO}_3\text{Me}^+ \times n\text{H}_2\text{O}$  surface species is treated as an outer-sphere complex with some water molecules between the  $\text{CO}_3^-$  surface site and hydrated  $\text{Me}^{2+}$  adsorbed cation. Indeed, a significant increase in the intensity of the  $3400\text{ cm}^{-1}$  band is observed at  $\text{pH} \approx 9$  for the samples equilibrated in 0.01 to 0.1 M  $\text{Ca}^{2+}$  or  $\text{Mg}^{2+}$  solutions as compared to the samples prepared without added metal ions (Figure 11, 12c). Note that in this region of pH, the concentration of  $>\text{MeOH}_2^+$  groups is very low (Figures 1, 11a, and 11e). Thus, the

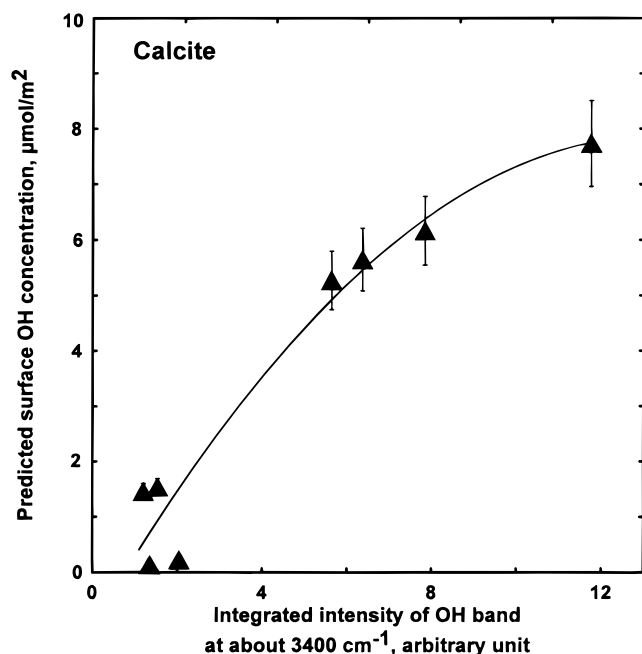


**Figure 7.** Relationship between the predicted surface hydroxyl concentration of calcite ( $>\text{CaOH}_2^+$ ) and the integral intensity of OH absorbance band at around  $3400\text{ cm}^{-1}$  in the region of stretching vibration. The line represents the empirical fit to the data.

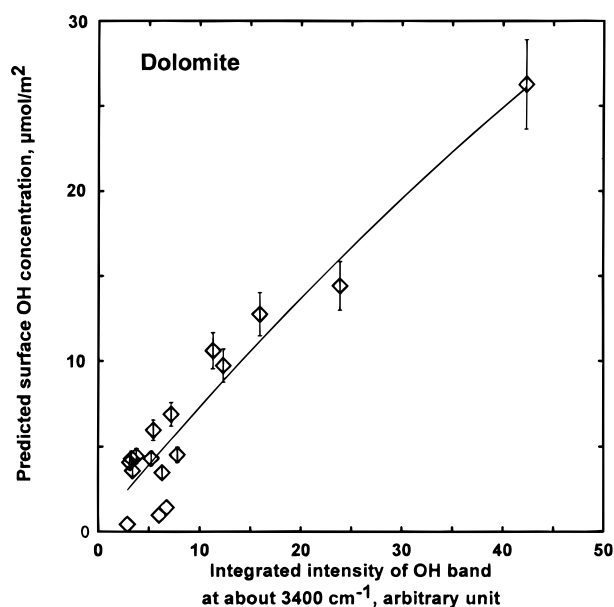


**Figure 8.** Relationship between the predicted surface hydroxyl concentration of dolomite ( $>\text{MgOH}_2^+ + >\text{CaOH}_2^+ + >\text{CO}_3\text{H}^0$ ) and the integral intensity of the OH absorbance band at around  $3400\text{ cm}^{-1}$  in the region of stretching vibration. The line represents the empirical fit to the data.

broad band at  $\sim 3400\text{ cm}^{-1}$  could be assigned almost entirely to water molecules surrounding the magnesium (Figure 11b–d) or calcium (Figure 11f, g) ions adsorbed from solution.

These findings are very different from those when the experiments were performed at low pH without adding magnesium to the solution. For example, in the absence of additional magnesium in solution the difference spectrum d (Figure 12d) after increasing solution pH from acidic to basic clearly shows a decrease of hydroxyl group surface density with a coincident increase of carbonate species surface density when the solution pH increases.

It should be also noted that the shape of the bands observed at lower pH, where the  $>\text{MeOH}_2^+$  surface group dominates (Figure 12d), is different from that found at higher pH in magnesium-rich solutions (Figure 12e) for which the density of the  $>\text{MeOH}_2^+$  surface groups is very low as compared to that of  $>\text{CO}_3\text{Mg}^+ \times n\text{H}_2\text{O}$ . This observation is in agreement with the postulated different origin of the OH stretching vibration absorbance bands at about  $3400\text{ cm}^{-1}$  depending on the hydration state.

Note that the effect of magnesium on the intensity of the band at  $3400\text{ cm}^{-1}$  is higher than that of calcium (Figure 11). This is explained in view of different hydration energies, and consequently, a different amount of water molecules attached to these two adsorbed cations.<sup>77</sup> This discussion implies that the adsorbed cations always stay hydrated on the surface. This is in contrast to the previous study of Mn adsorption on  $\text{FeCO}_3$ <sup>78</sup> where it has been shown that a progressive dehydration of the sorbed cation occurs over the course of 7 days. This time is much longer than the preequilibration procedure applied in this study (i.e., 24 h). Therefore, we assume that the dehydration of the adsorbed Ca and Mg is negligible in our experiments.

**Structural Features of Hydrated Calcite and Dolomite Surfaces.** The model of calcite and dolomite surface chemistry presented in this study is based on an unrelaxed and unreconstructed surface and, therefore, should be considered as a preliminary description of the actual surface.<sup>18,79</sup> The dominant crystal planes are {1014} for calcite and {1014, 1011, and 1120} for dolomite<sup>80</sup> although the solution composition can influence microtopographic characteristics of surfaces and the appearance of different forms. Besides, it has been argued that hydration leads to the formation of a thick, disordered or amorphous hydrated surface layer.<sup>81</sup> However, this was not confirmed by XPS and LEED studies<sup>28</sup> that show the presence of an ordered surface at least  $10\text{ Å}$  thick that is very similar to the bulk solid.

The {1014} face of calcite is a nonpolar surface with cationic  $\text{Ca}^{2+}$  and anionic  $\text{CO}_3^{2-}$  groups connected via a rhombohedral network, and oxygen atoms both  $0.8\text{ Å}$  above and below the surface, as well as in the surface plane. Atomistic simulation calculations for the three calcite planes {1014, 1011, and 1120} show that the water molecules are adsorbed uniformly on equivalent surface sites.<sup>4</sup> They lie flat on the surface with one oxygen atom coordinated to the surface calcium ion at a distance of  $2.37\text{ Å}$  and two hydrogens pointing toward two surface oxygen ions. For the {1011} calcite surface, the oxygen of the water molecule is coordinated to surface calcium ions at  $2.33\text{ Å}$  and to surface oxygens by one hydrogen at  $1.69$  or  $1.80\text{ Å}$ ; for the {1120} calcite surface, the oxygen atom of the adsorbed water molecule coordinates to two surface calcium ions at  $2.69$  and  $2.75\text{ Å}$  while one of its hydrogen atoms coordinates to lattice oxygen at  $2.05\text{ Å}$ .<sup>4</sup>

Further atomistic simulation calculations revealed that the  $\text{CO}_3$  terminated face {1014} for calcite is the most stable whereas for dolomite, Ca- and Mg-terminated {1010} and {1120} faces are also important.<sup>5</sup> This may explain the higher concentration of hydroxyl-bearing species ( $>\text{MeOH}_2^+$ ) in the surface spectra of dolomite

(77) Burgess, J. *Ions in Solutions: Basic Principles of Chemical Interactions*; Ellis Horwood Ltd. 1988.

(78) Wersin, P.; Charlet, L.; Karthein, R.; Stumm, W. *Geochim. Cosmochim. Acta* **1989**, *53*, 2787.

(79) Staudt, W. J.; Reeder, R. J.; Schoonen, M. A. A. *Geochim. Cosmochim. Acta* **1994**, *58*, 2087.

(80) Fouke, B. W.; Reeder, R. J. *Geochim. Cosmochim. Acta* **1992**, *56*, 4015.

(81) Davis, J. A.; Fuller, C. C.; Cook, A. D. *Geochim. Cosmochim. Acta* **1997**, *51*, 1477.

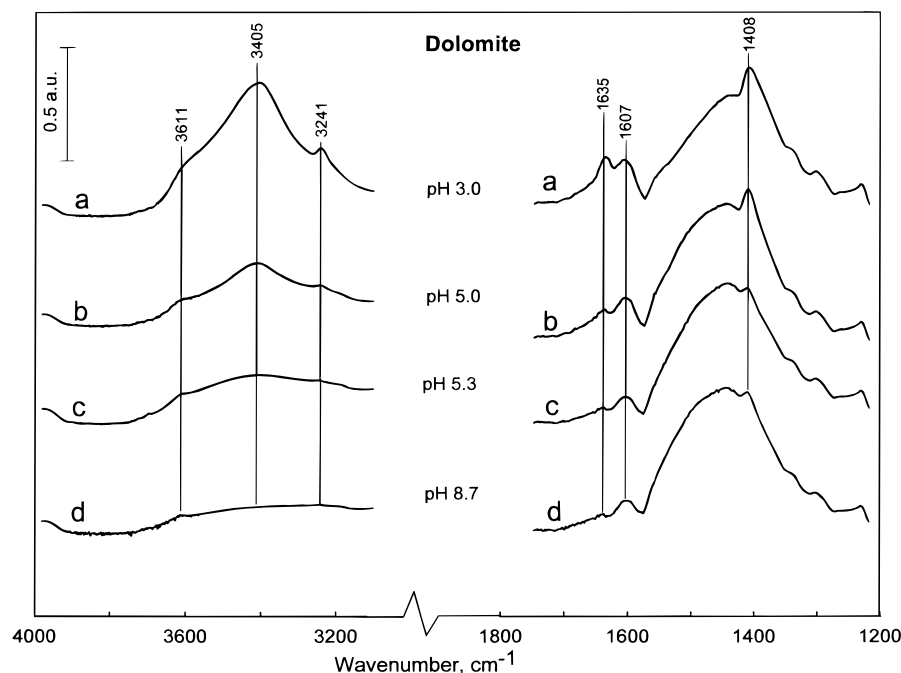


**Figure 9.** DRIFT spectra of dolomite samples after contact with different solutions. (a) D1; (b) D2; (c) D3; (d) D10.

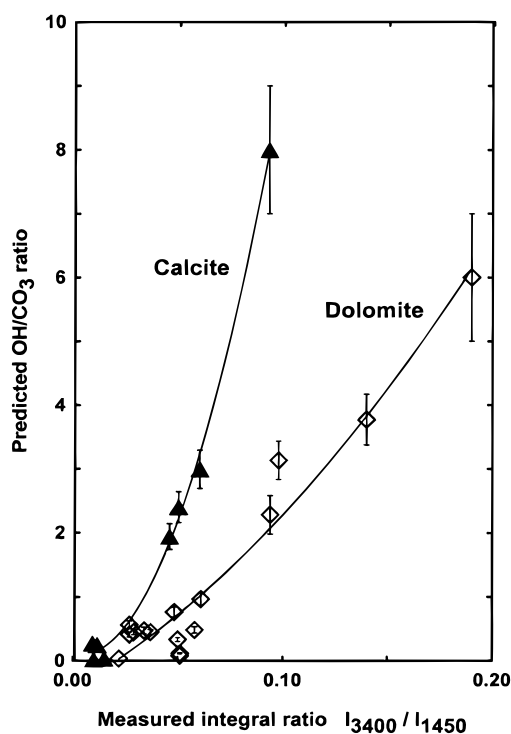


**Figure 10.** Predicted surface concentration ratio  $[\text{OH}]_{\text{total}}/[\text{CO}_3]_{\text{total}}$  versus experimentally measured band integrated intensities ratio  $I_{3400}/I_{1420}$  for calcite and dolomite. The lines represent the best fits to these empirical dependencies.

compared to that of calcite observed in this study. Although the fundamental surface coordination is similar for calcite and dolomite, the main surface structural difference between these minerals arises from the presence of stepped  $\{1011\}$  and  $\{1120\}$  forms on dolomite compared to the sole  $\{1014\}$  form for calcite, as shown by periodic bond chain modeling<sup>80</sup> in agreement with observations of natural samples.<sup>82,83</sup> These differences are primarily

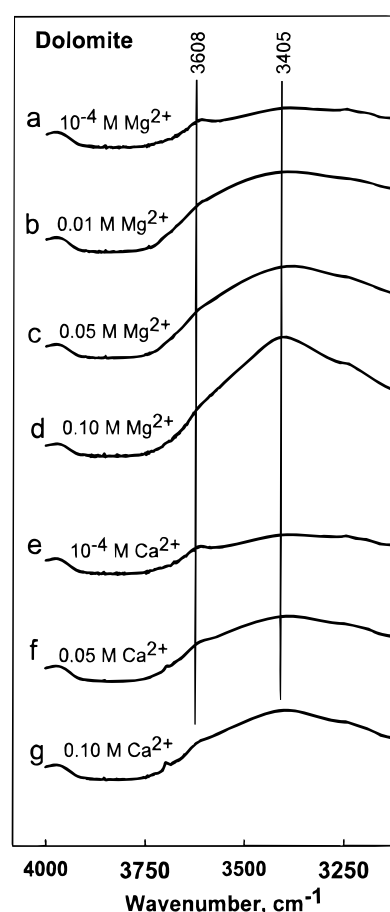


**Figure 11.** DRIFT spectra of dolomite samples after contact with Ca- and Mg-bearing solutions at  $\text{pH} \approx 9$ : (a) D12; (b) D18; (c) D19; (d) D20; (e) D12; (f) D21; (g) D22.

responsible for the different surface composition of different crystal planes and their different reactivities in solution. In particular, the higher concentration of cations on dolomite stepped and kink surfaces (mostly  $\{1011\}$  and  $\{1120\}$  planes) leads to a higher amount of coordinated

(82) Reeder, R. J.; Protsky, J. L. *J. Sediment. Petrol.* **1986**, 56, 237.

(83) Kretz, R. *Am. Mineral.* **1988**, 73, 619.

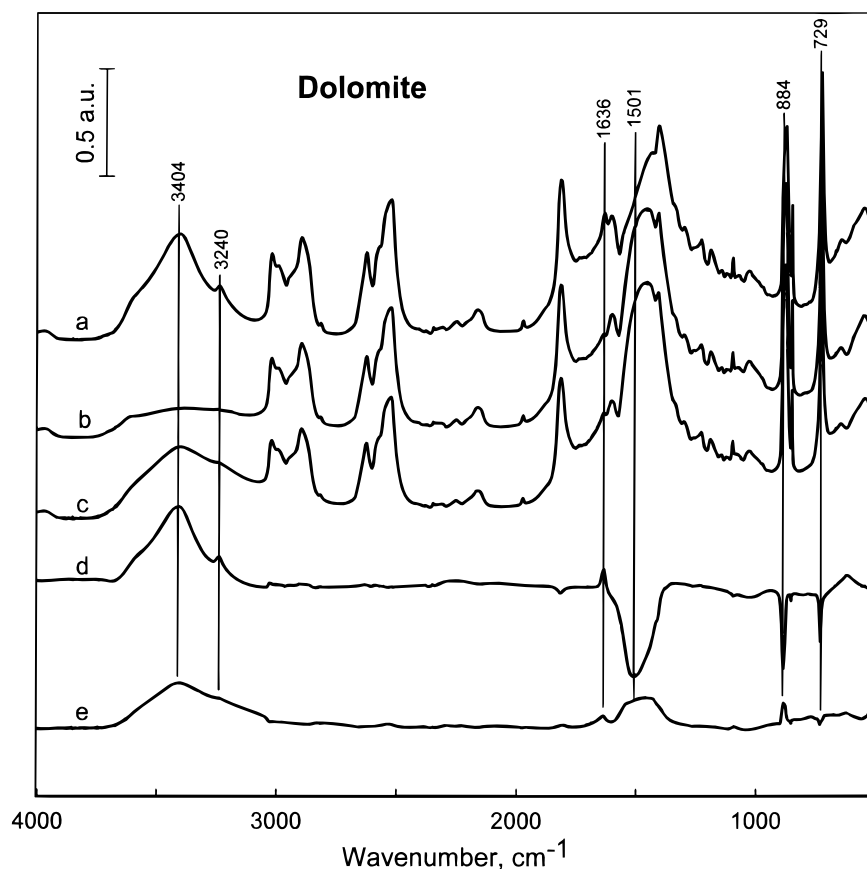


**Figure 12.** DRIFT spectra of dolomite samples in acidic to neutral solutions and Mg-rich alkaline solutions: (a) D1, pH = 3.0; (b) D9, pH = 7.75; (c) D20, pH = 8.9 and  $[Mg^{2+}] = 0.1$  M; (d) difference spectrum (D1)–(D9); (e) difference spectrum (D20)–(D9).

water molecules raising the intensity of the OH infrared bands observed in the present study for this mineral. The increase of growth rates for {1011} sectors relative to {1014} for dolomite<sup>80</sup> is in agreement with a control of carbonate reactivities in aquatic systems by surface metal hydration.<sup>61,65</sup>

It should be noted in conclusion that the surface structural features of calcite and dolomite such as different faces and kink sites described by Reeder et al.,<sup>18,20,79,80</sup> imply that the geometry, coordination, and "size" of surface sites are defined by the structure-bound anhydrous ions such as Me or CO<sub>3</sub> groups, whereas in the SCM used in this study, such surface groups are hydrated metal ( $>MeOH_2^+$ ) or negatively charged carbonate ( $>CO_3^-$ ) species. Their distribution on the kink sites and stepped forms should be similar to that of the nonhydrated surface as is the case for the dominant {1014} cleavage plane. Additional infrared reflection studies on different hydrated carbonate crystal planes are necessary to evaluate the surface structural control on the mineral surface speciation in aqueous solutions.

**Sources of Uncertainties.** There are two major sources of experimental uncertainty associated with possible alteration of the surface composition of the samples treated in basic solutions during their preparation for spectroscopic surface characterization: (i) a deposition of salts from solution during emersion of sample and drying, and (ii) an atmospheric CO<sub>2</sub> adsorption on wet mineral surfaces. Close analysis of the infrared spectra allows us to conclude that these effects are negligible when compared with the original surface composition of minerals generated by modification of solution conditions.

If deposition of dissolved components from solution would be significant, the measured surface concentration

of, for example, OH groups should be proportional to NaOH concentration in solution. As shown in Figures 5, 6, and 9, the opposite relationship is observed in the recorded spectra as the concentration of surface OH groups decreases with increasing solution pH.

It has been argued that because all calcite surfaces in air are covered by a capillary layer of water,<sup>84</sup> this water layer quickly becomes saturated with respect to calcite and the contacting atmospheric CO<sub>2</sub>.<sup>85</sup> As a result, the surface species distribution should reflect equilibrium with the bulk solid and there should be no influence due to conditioning in different solution. Hence, the increase of the surface OH group concentration with decreasing pH documented in this study would not be possible if at any solution pH the surface films were in equilibrium with the bulk solid. This equilibrium condition should correspond to the pH at the point of zero charge (pH<sub>PZC</sub>) when the concentration of the ( $>MeOH_2^+$ ) and ( $>MeCO_3^-$ ) species is the same and pH independent. Note also that in the spectrophotometer chamber (purged by dry CO<sub>2</sub> free air), where the mineral samples are dried, CO<sub>2</sub> concentration is much lower than in the ambient atmosphere at which the samples were equilibrated. Therefore, any artificial increase in the surface CO<sub>3</sub> group concentration during sample drying and collection of spectroscopic data is unlikely.

These experimental observations indicate that the surface speciation imposed by solution conditions is stable at least in the time frame of the performed characterization of mineral surfaces.

(84) Chiarello, R. P.; Wogelius, R. A.; Sturchio, N. C. *Geochim. Cosmochim. Acta* **1993**, *57*, 4103.

(85) Stipp, S. L. S.; Gutmannsbauer, W.; Lehmann, T. *Amer. Mineral.* **1996**, *81*, 1.



### Conclusions

The experimental results show that it is possible to monitor by infrared diffuse reflectance techniques the surface hydroxyl and carbonate groups on calcite and dolomite powders after their contact with aqueous solutions at different pH values, and carbonate and  $\text{Me}^{2+}$  concentrations. Major changes in the recorded spectra assigned to the variation in mineral surface composition were observed in two spectral regions. The band at around  $3400\text{ cm}^{-1}$  was attributed to the presence of  $>\text{CaOH}_2^+$  and  $>\text{MgOH}_2^+$  hydroxyl-containing surface species. The second region around  $1400\text{ cm}^{-1}$  is characteristic for carbonate surface (and bulk) groups. Both for calcite and dolomite, very good relationships were observed between the predicted concentration of the surface OH and  $\text{CO}_3$  groups and the intensities of the corresponding hydroxyl

and carbonate bands of the IR spectra. This study provides direct evidence for the existence of the different hydroxyl and carbonate surface species demonstrating the validity of the surface complexation approach in describing the chemistry of the carbonate mineral/aqueous solution interfaces. It is anticipated that such an approach can be applied for the spectroscopic evaluation of surface complexes for other metal carbonates. Note, however, that full spectroscopic quantification of all present surface species would require the use of isotopically labeled aqueous solutions and solid phases.

**Acknowledgment.** We thank Laurent Charlet and seven anonymous reviewers for valuable and insightful comments.

LA980905E